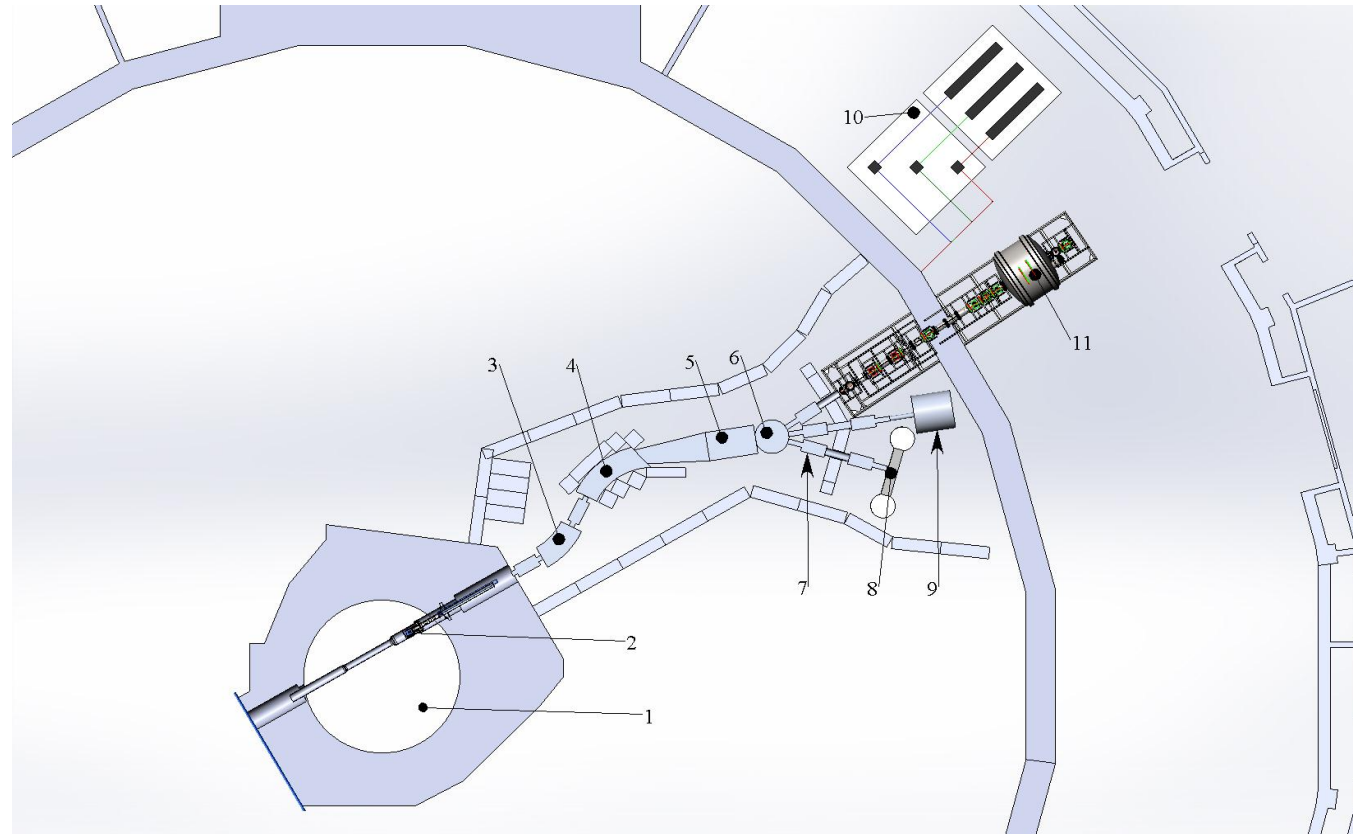


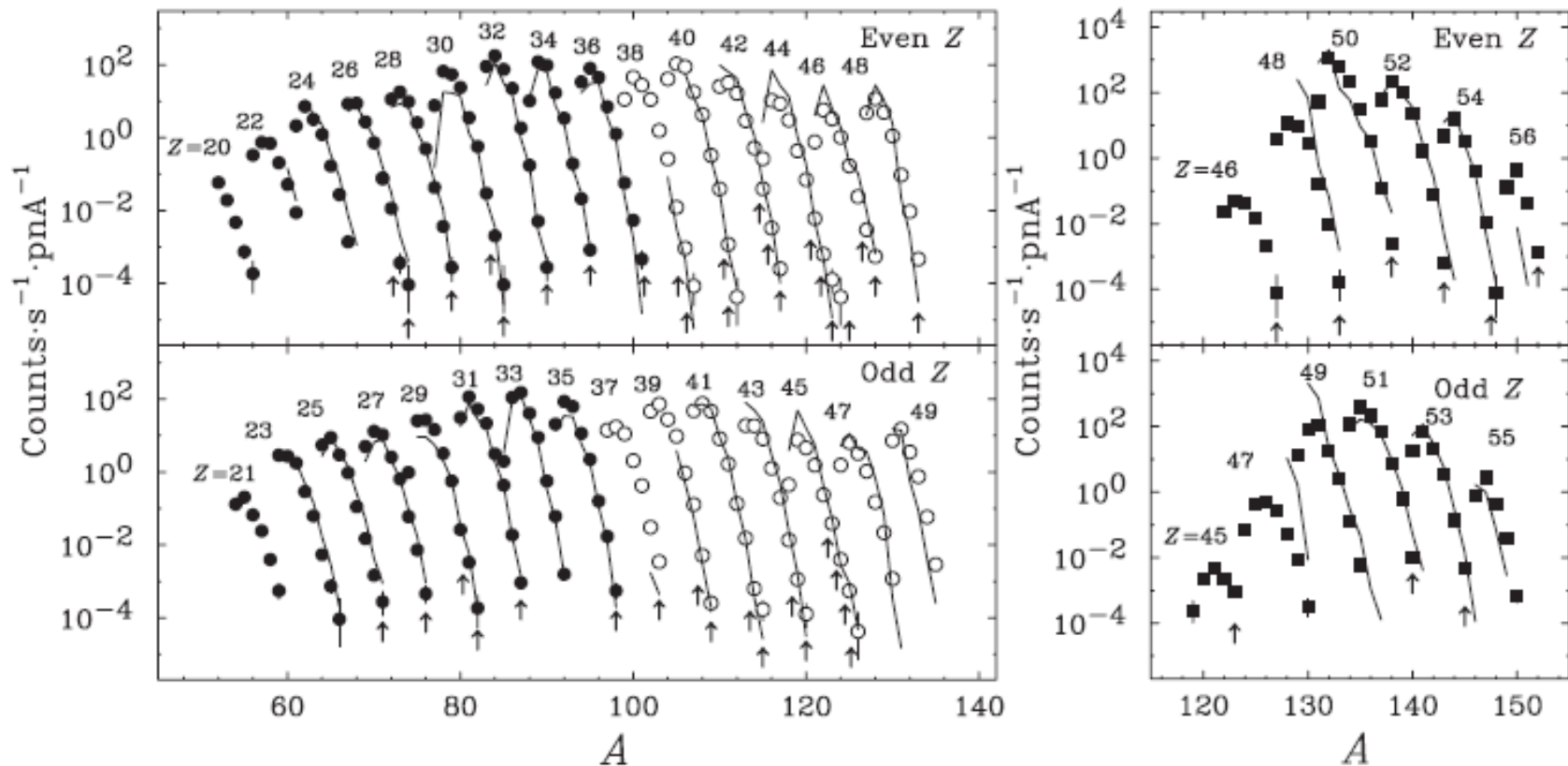
Проект ИРИНА: Лазерная (ядерная) спектроскопия на реакторе ПИК

IRINA



1. Корпус реактора ПИК с радиационной защитой. 2. Мишенно-ионное устройство с электростатической ионно-оптической системой. 3. Поворотная система ионного пучка. 4. Магнит масс-сепаратора. 5. Дисперсионная и коллекторная камеры. 6. Камера разводки ионных пучков. 7. Ионные тракты. 8. Лентопротяжное устройство. 9. Нейтронный детектор. 10. Лазерная установка. 11. Комплекс ионных ловушек (ПИТРАП).

RIKEN: Yields



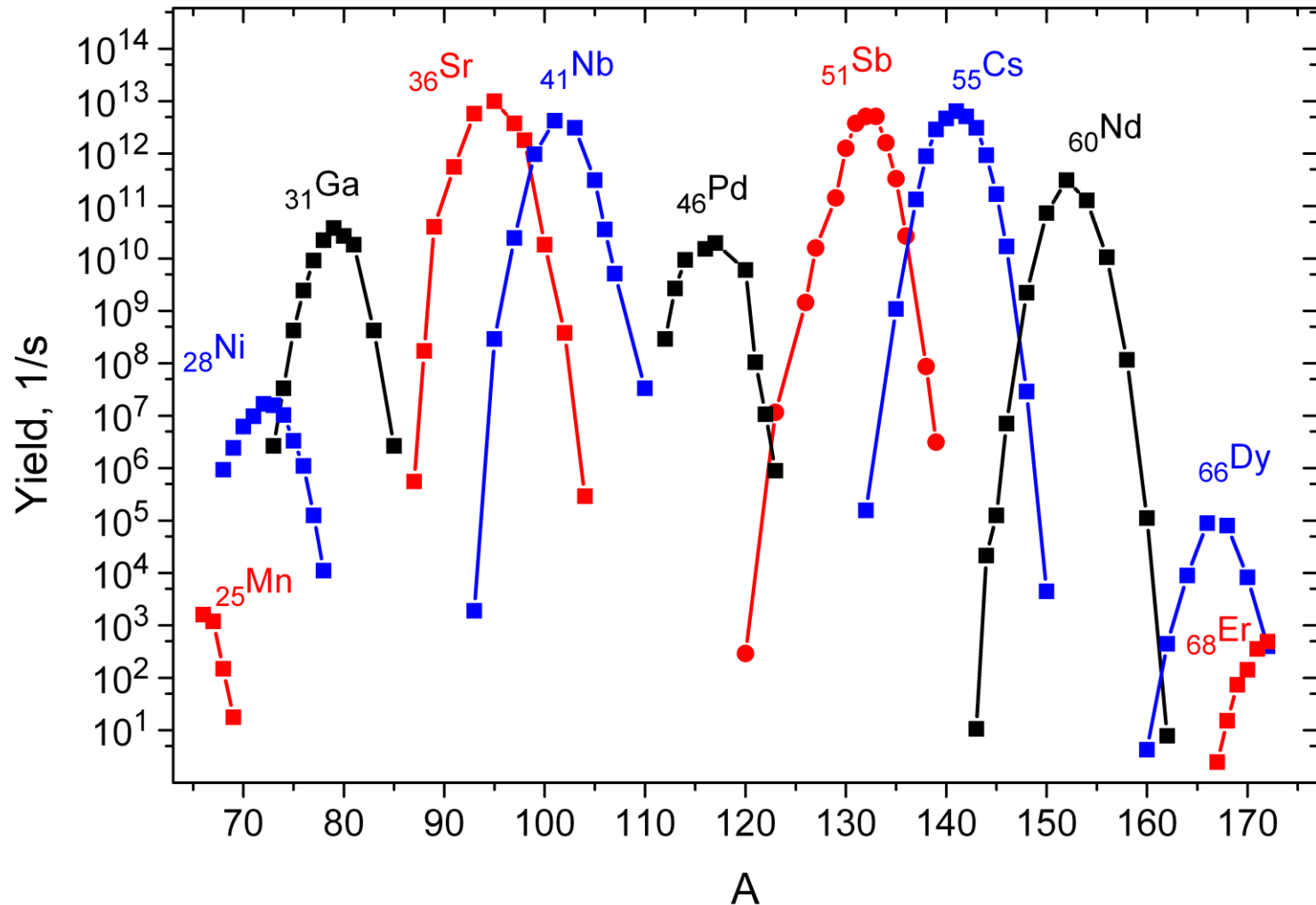
RIKEN-RIBF (Radioactive Isotope Beam Factory)

$T_{1/2}$ for $^{78,79,80}\text{Ni}$, $^{76,77}\text{Co}$, $^{80,81}\text{Cu}$: Z. Y. Xu et al., PRL 113, 032505 (2014)

T. Ohnishi et al., Phys. Soc. Jap. 79, 2010, 073201

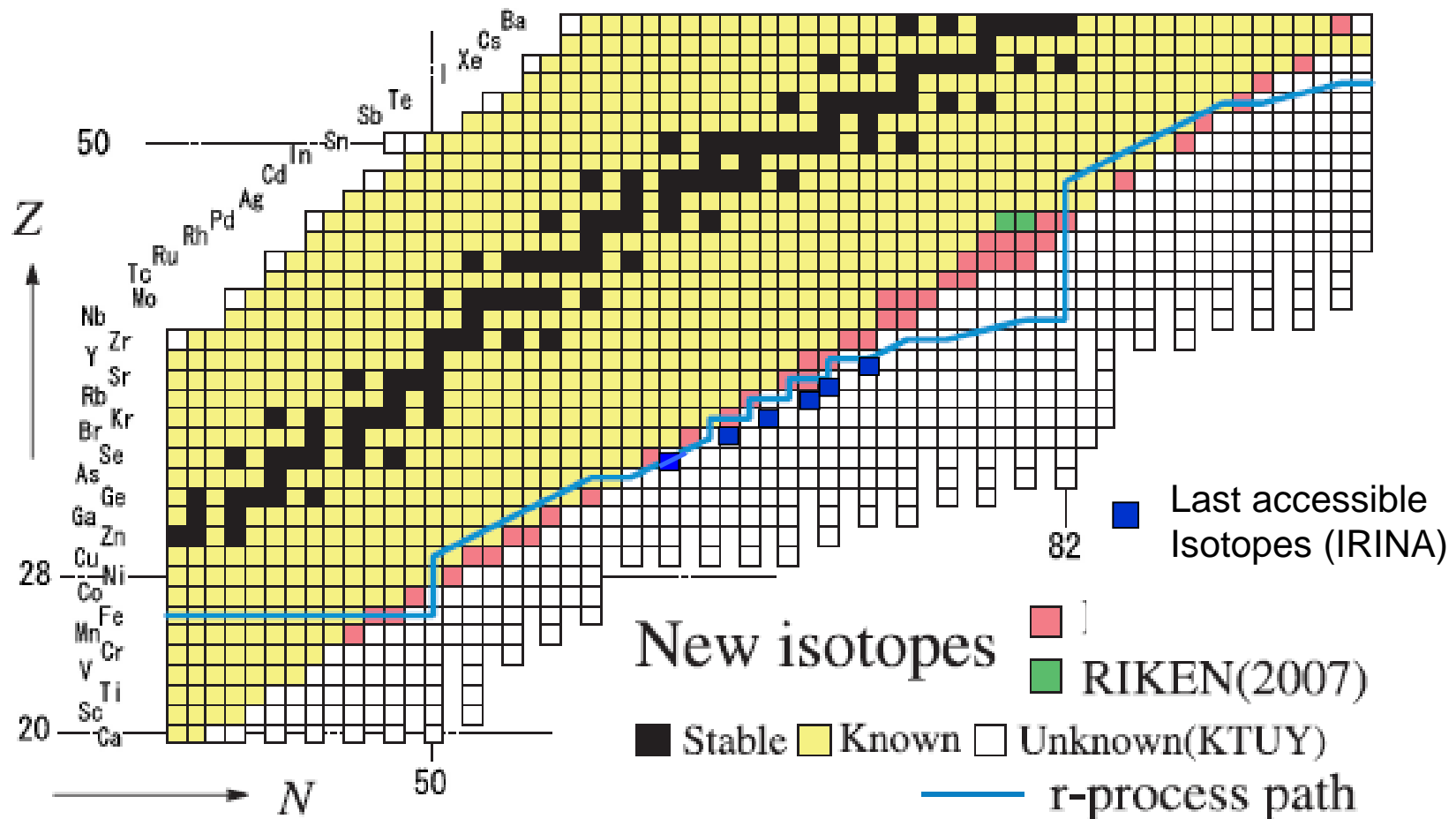
IRINA: Yields

Yields were calculated with 5 g of ^{235}U in target and 3×10^{13} n/cm 2 /s

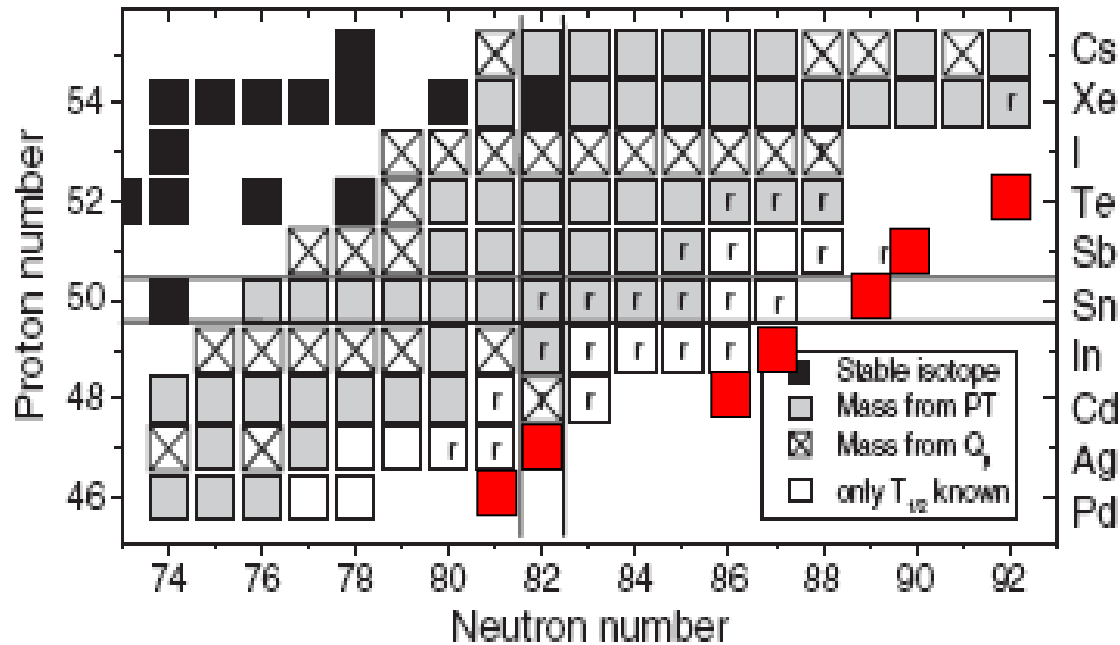


IRINA: r-process

Values needed for r-process calculations: $T_{1/2}$, β -n branchings



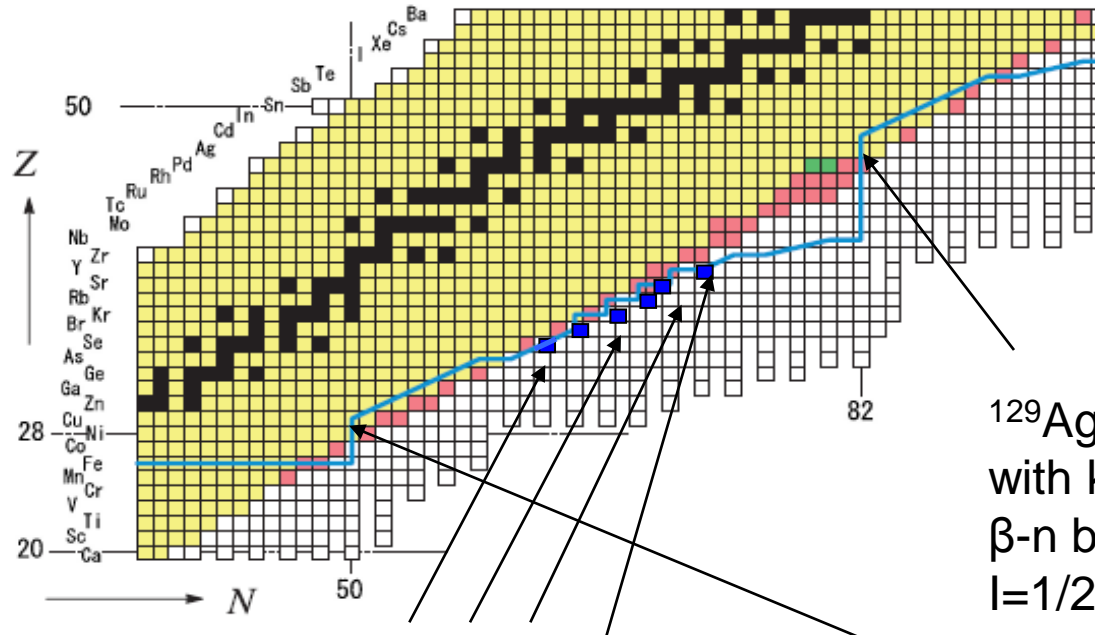
IRINA: r-process



■ Last accessible at IRINA

J. Hakala et al., Phys. Rev. Lett. 109, 032501 (2012)

IRINA: r-process

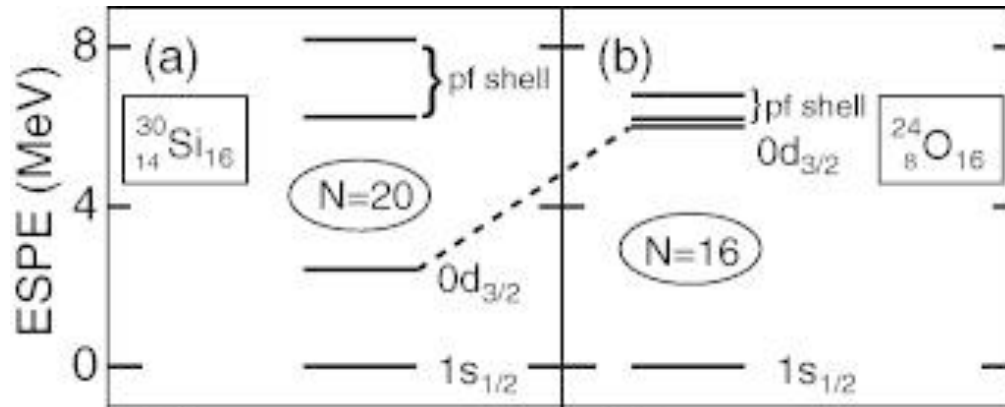


$^{95}\text{Se} \sim 10^2$, $^{98}\text{Br} \sim 10^3$, $^{101}\text{Kr} \sim 10^4$,
 $^{103}\text{Rb} \sim 10^5$ (RIKEN-RIBF ~ 50),
 $^{106}\text{Sr} \sim 10^3$, $^{109}\text{Y} \sim 10^3$

^{129}Ag , ^{78}Ni : waiting points
 with known $T_{1/2}$ and unknown
 β -n branchings. $T_{1/2}$ for ^{129}Ag
 $I=1/2$ isomer and its excitation
 energy are not known.
 Expected yields $^{129}\text{Ag} \sim 1$ 1/s;
 $^{78}\text{Ni} \sim 10^4$ 1/s

(RIKEN: $^{238}\text{U} + \text{Be}$, 345 MeV/n, 6×10^{10} 1/s — 10^4 ^{78}Ni in 13 days)

Shell evolution for exotic nuclei



Neutron single particle energies for (a) ^{30}Si and (b) ^{24}O , relative to $1s_{1/2}$.

Shell evolution:

^{24}O — new magic number at $N=16$,

^{54}Ca — new magic number at $N=34$,

disappearance of the $N=20$ (^{32}Mg) and 28 (^{42}Si) shell gaps, etc.

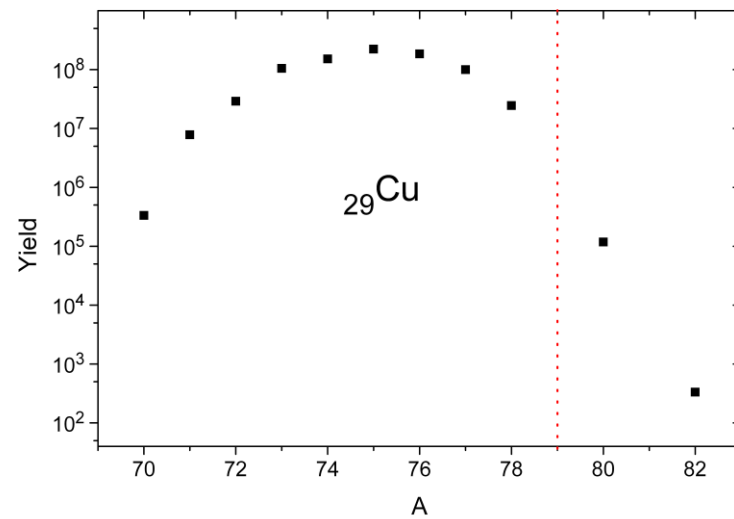
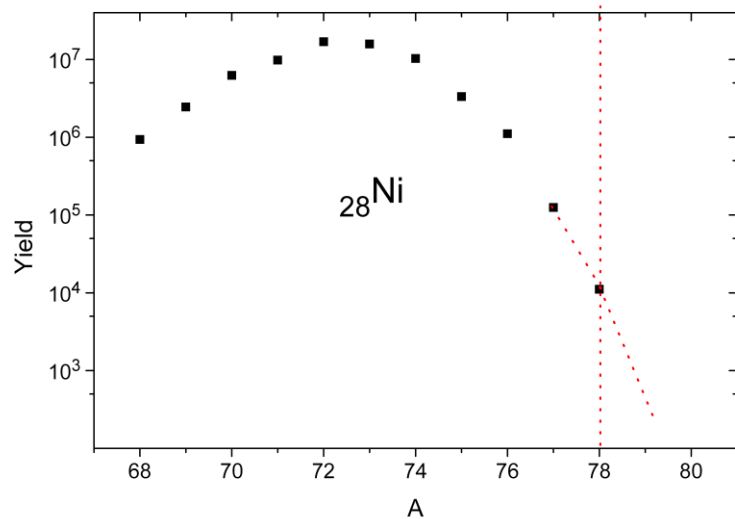
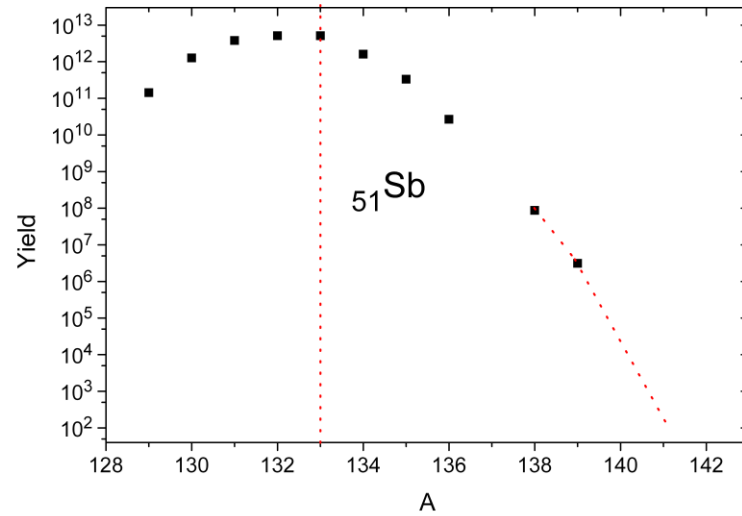
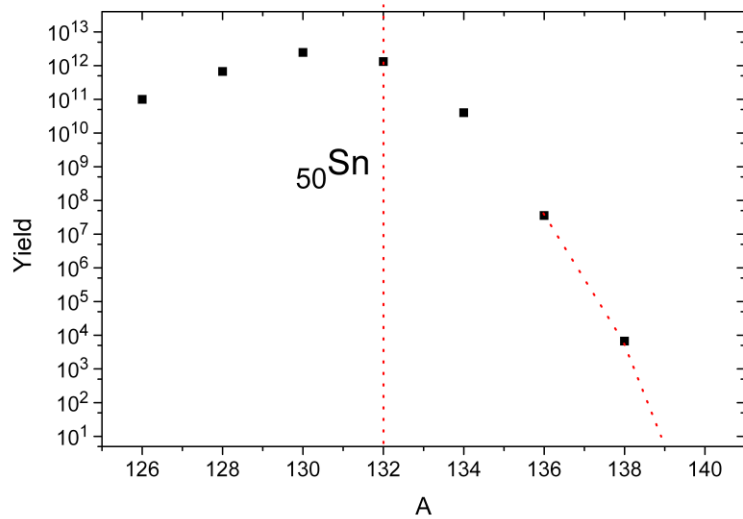
It was explained by introducing **tensor forces** or/and **$3N$ forces**

For O the drip line is strikingly close to the stability line (last bound is doubly magic ^{24}O ; cf. last bound ^{31}F , $Z=8+1$).

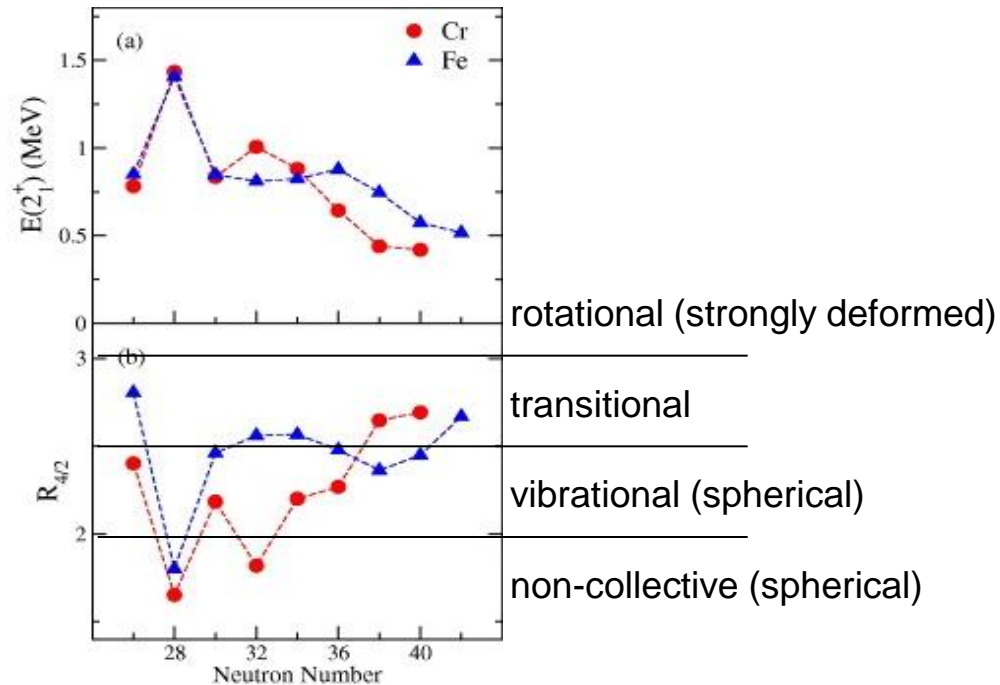
This phenomenon was explained by introducing **$3N$ forces**.

(See EFT studies with naturally arisen $3N$ forces: E. Epelbaum et al., RMP, 81 (2009) 1773)

IRINA: Yields



Disappearance of N=40 sub-shell



The different behavior of excitation energies for these Cr and Fe isotopes point to a different intrinsic structure for the two $N = 40$ isotones. These observations represent a challenge for the most modern nuclear interactions.

$E(2^+)$ and $R(E_{4^+}/E_{2^+})$ systematics for neutron-rich ^{24}Cr and ^{26}Fe isotopes in the range $26 \leq N \leq 40$.

IRINA: disappearance of N=40 shell

Calculations: ground states of all the Fe isotopes are predominantly of spherical character, whereas ground states of $^{62,64}\text{Cr}$ are dominated by a deformed configurations.

Striking similarity with Pb region: shape coexistence predicted.

$$^{67}\text{Co}^{40} \sim 4.5 \times 10^5 \text{ 1/s}$$

$$^{65}\text{Mn}^{40} \sim 10^4 \text{ 1/s}$$

$$^{69}\text{Mn}^{44} \sim 20 \text{ 1/s}$$

$$^{64}\text{Cr}^{40} \sim 10 \div 100 \text{ 1/s}$$

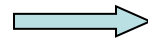
$$^{66}\text{Fe}^{40} \sim 8 \times 10^4 \text{ 1/s}$$

$$^{73}\text{Fe}^{47} \sim 10 \text{ 1/s}$$

Previously measured

Achievable at IRINA

54-58 Fe^{28-32}



up to N=46

50-56 Mn^{25-31}



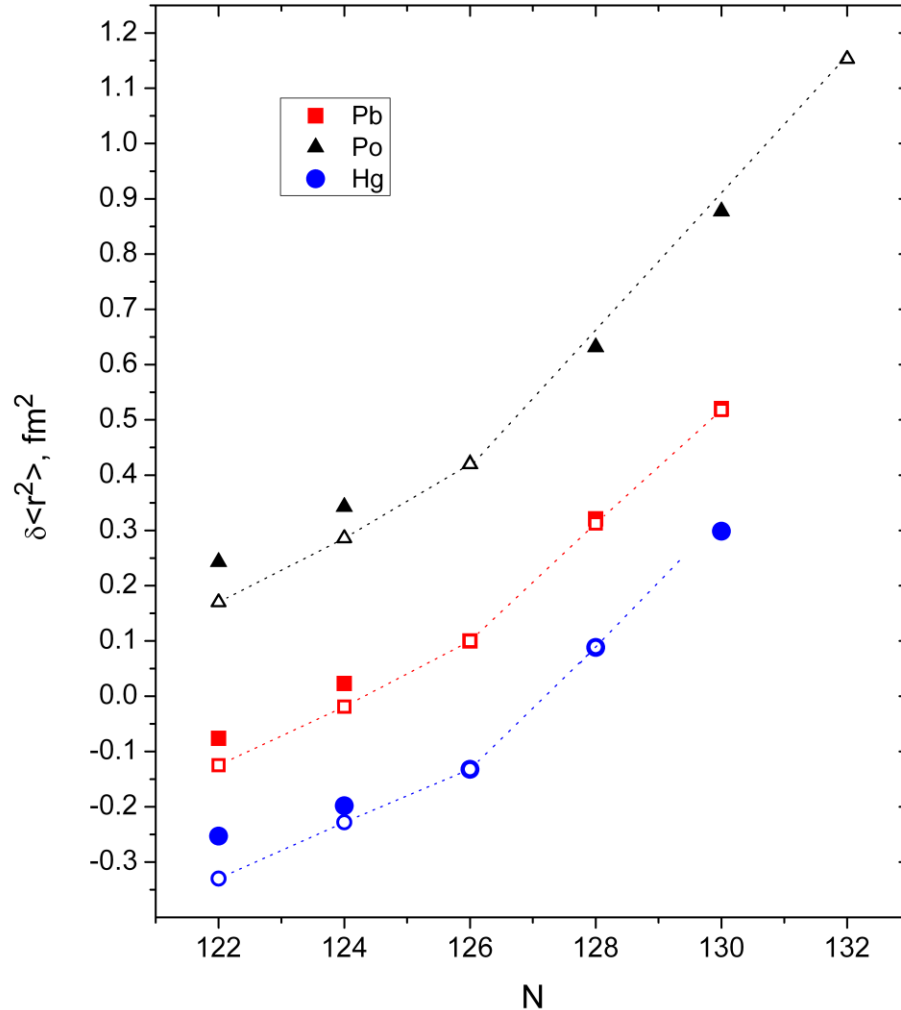
up to N=44

50-54 Cr^{26-30}



up to N=40

Shell-effect in radii at $N=126, Z=82$

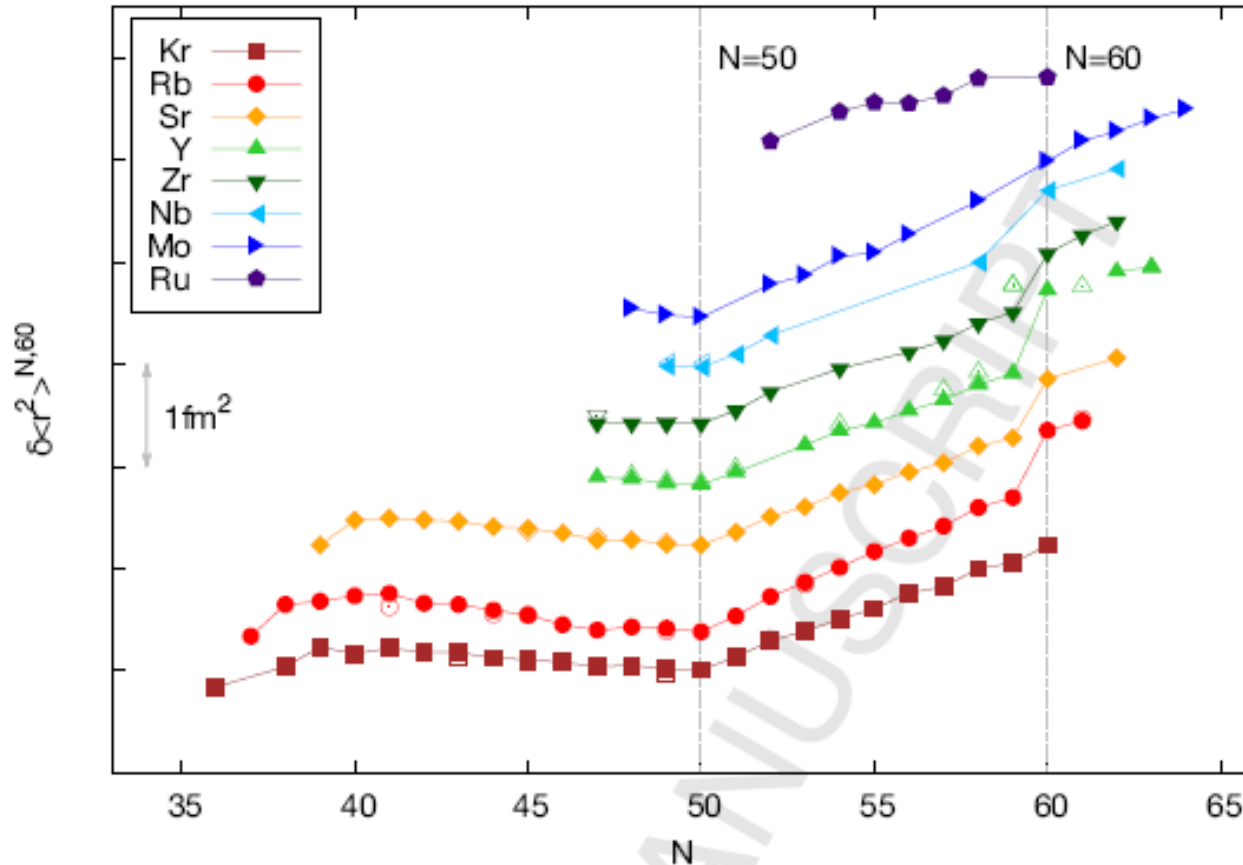


Hollow symbols —
experiment

Full symbols —
RMF calculations

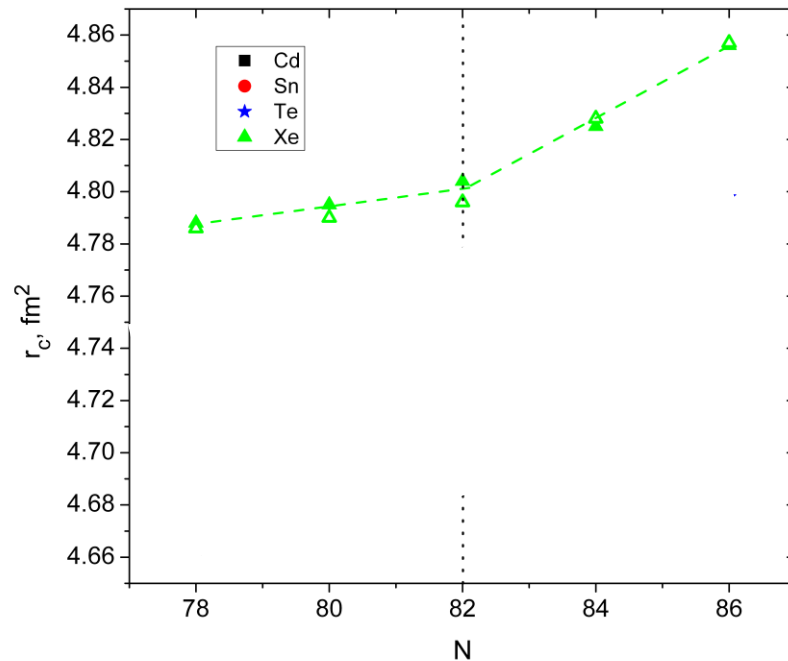
(σ scalar, isoscalar
 ρ vector, isovector
 ω vector, isoscalar)

Shell-effect in radii at N=50

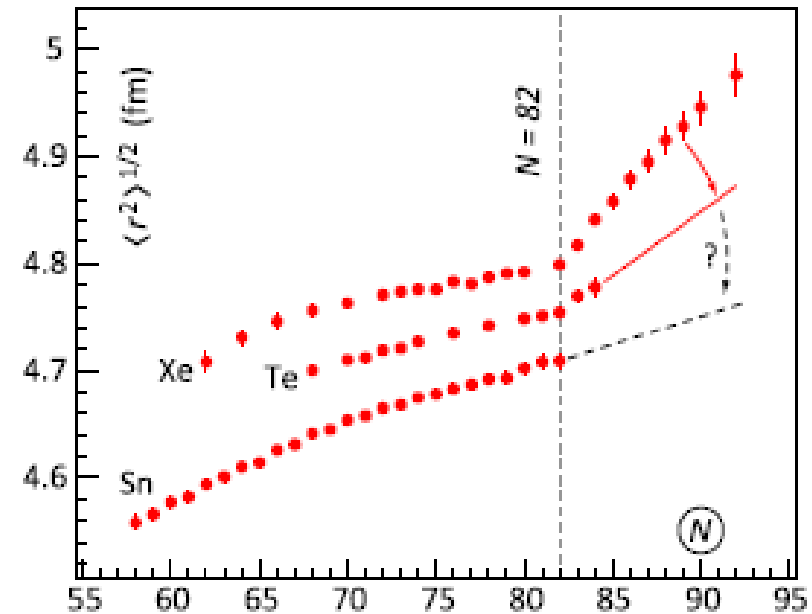


The same kink in Ga (very n-rich)

IRINA: shell-effect in radii at N=82, Z=50



theory (RMF)



experiment

G. A. Lalazissis et al., ADNDT 71, 1 (1999)

Previously measured

Achievable at IRINA

102-129Cd⁵⁴⁻⁸¹



up to N=86

104-127In⁵⁵⁻⁷⁸



up to N=87

108-132Sn⁵⁸⁻⁸²



up to N=89

(Sb)



N=69-90

120-136Te⁶⁸⁻⁸⁴

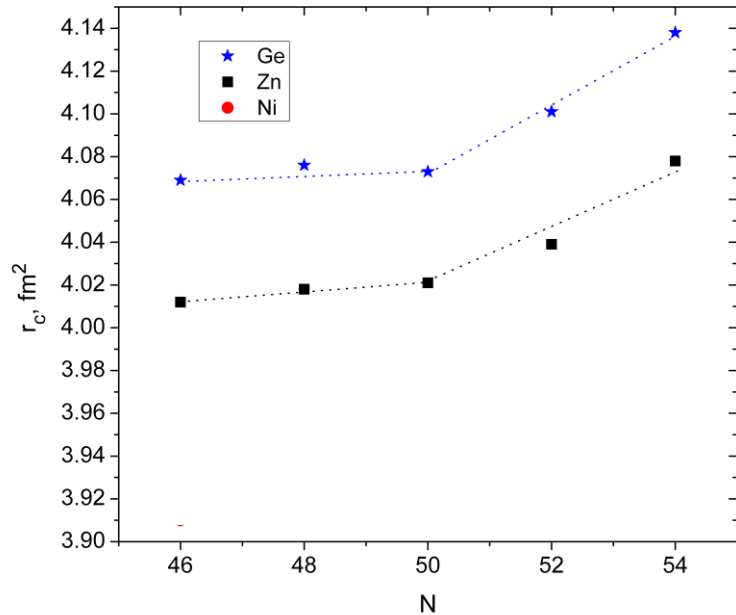


up to N=92

N>88 — classical deformation region!

New shell closure at N=90, Z~50 is predicted.

IRINA: shell-effect in radii at N=50, Z=28



theory (RMF)

Achievable at IRINA

^{28}Ni up to $N=52$

^{30}Zn up to $N=56$

^{32}Ge up to $N=57$

Previously measured

Achievable at IRINA

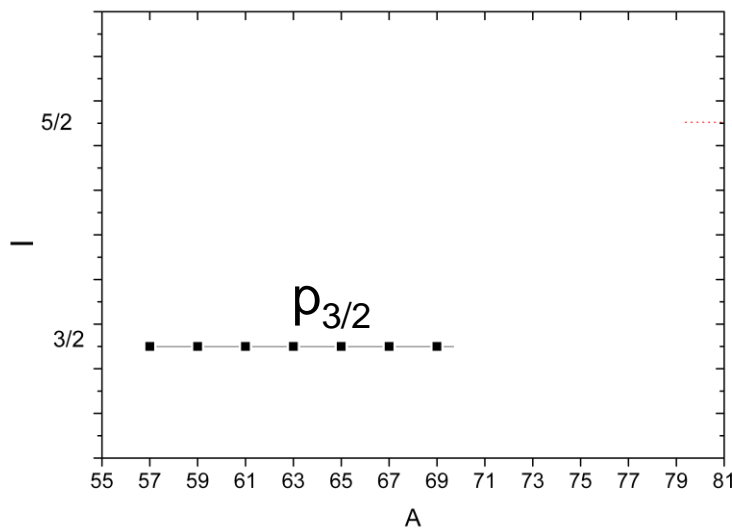
$^{63-82}\text{Ga}$



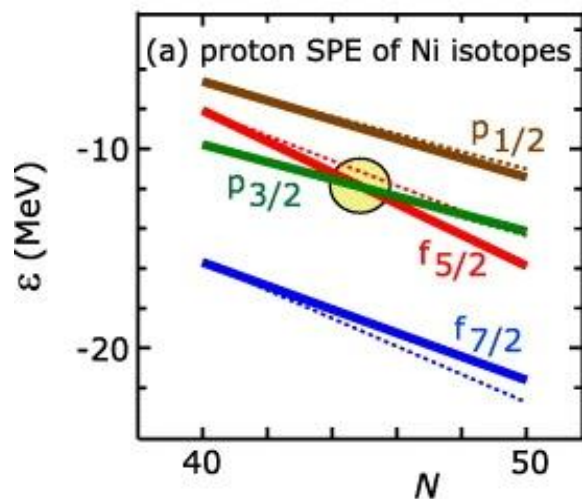
$^{32-51}$ up to $N=56$

G. A. Lalazissis et al., ADNDT 71, 1 (1999)

Shell evolution for exotic nuclei



spins for odd ${}_{29}\text{Cu}$ isotopes



SPEs of protons for Ni isotopes

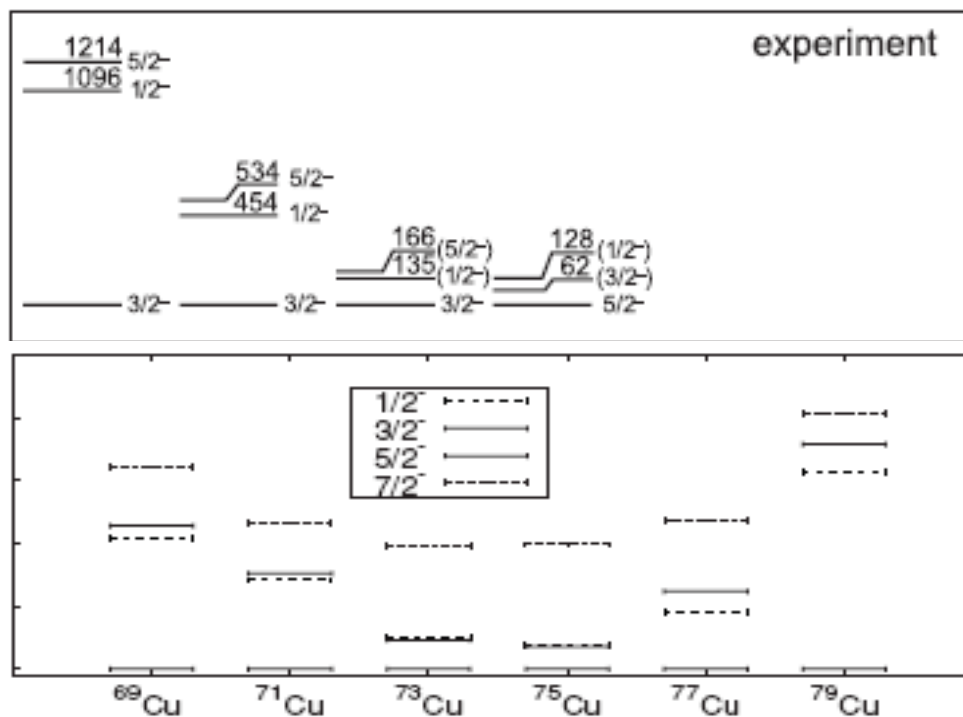
$f_{5/2} / p_{3/2}$ inversion was shown by I and μ laser measurements (${}^{71,73,75}\text{Cu}$) and may be explained with **tensor force** inclusion. (See also shell quenching)

It is of importance to trace the proton shell evolution beyond $N=50$.

Same inversion was found for Ga ($A=79-81$, $N=48-50$).

Shell evolution for exotic nuclei

K. T. Flanagan et al., PRL 103, 142501 (2009)

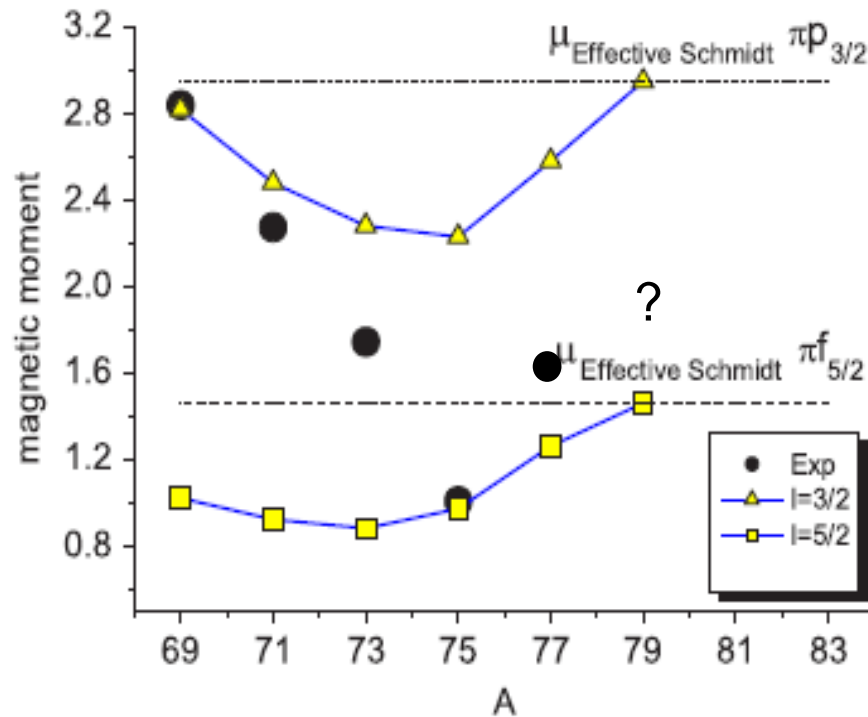


Lowering of $p_{1/2}$ state was reproduced only after Z=28 shell quenching taking into account

K. Sieja and F. Nowacki, Phys. Rev. C **81**, 061303 (2010)

Shell evolution for exotic nuclei

K. T. Flanagan et al., PRL 103, 142501 (2009); U. Köster et al., PRC **84**, 034320 (2011)

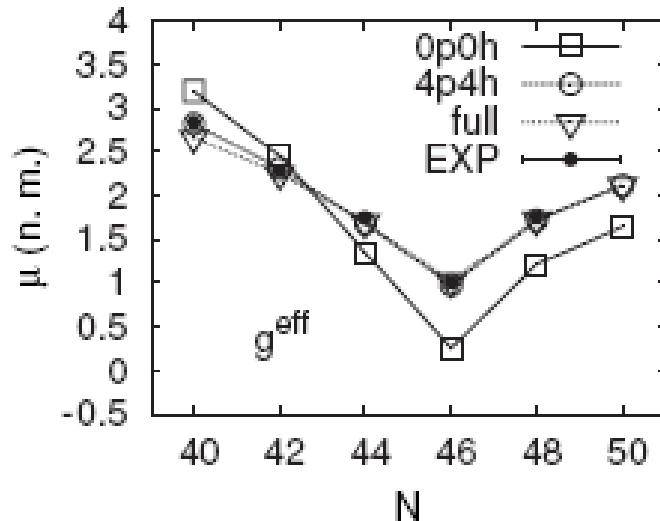


Unexplained lowering of $p_{1/2}$ state is responsible for the discrepancy between theory and experiment for $\mu(^{71,73}\text{Cu})$

Disagreement for $\mu(^{77}\text{Cu})$?

IRINA: Shell evolution for exotic nuclei

K. Sieja and F. Nowacki, Phys. Rev. C **81**, 061303 (2010).



$\mu(^{77}\text{Cu})$ may be reproduced only with Z=28 shell quenching by 0.7MeV

Previously measured Achievable at IRINA

57-78Cu²⁹⁻⁴⁹ → up to N=53

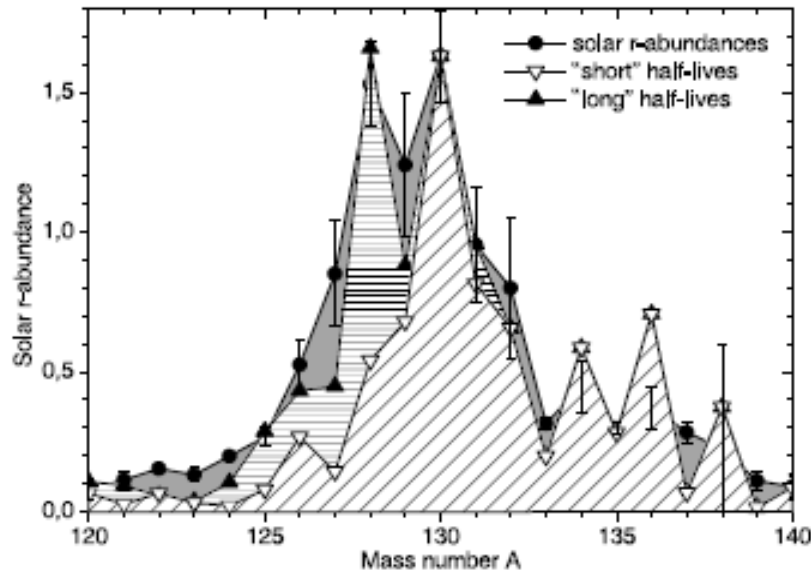
63-82Ga³²⁻⁵¹ → up to N=56

Note: rapid onset of deformation is expected beyond N=50; $T_{1/2}$ for ^{86,87}Ga are needed for r-process studies (shell quenching)

Whether the similar inversion occurs for Z=50 shell? Some indications of “tensor force induced” shell evolution was found in ¹²⁶Pd⁸⁰: small difference between the 10⁺ and 7⁻ isomers was ascribed to the tensor force shift of the 1h_{11/2} neutron orbit (H. Watanabe *et al*, PRL 113, 042502 (2014)). See also: J. Shergur *et al.*, Eur. Phys. J. A 25, 121 (2005) (5/2⁺ state in ¹³⁵Sb)

Quenching of the N=82 shell gap?

I. Dillmann et al., PRL 91, 162503 (2003)



Quenching of N=82 shell describes big $Q_\beta(^{130}\text{Cd})$, high energy of 1^+ state in ^{130}In and corresponding $\log(ft)$. Cf. also improvement of solar r-abundances at $A=130$ descriptions

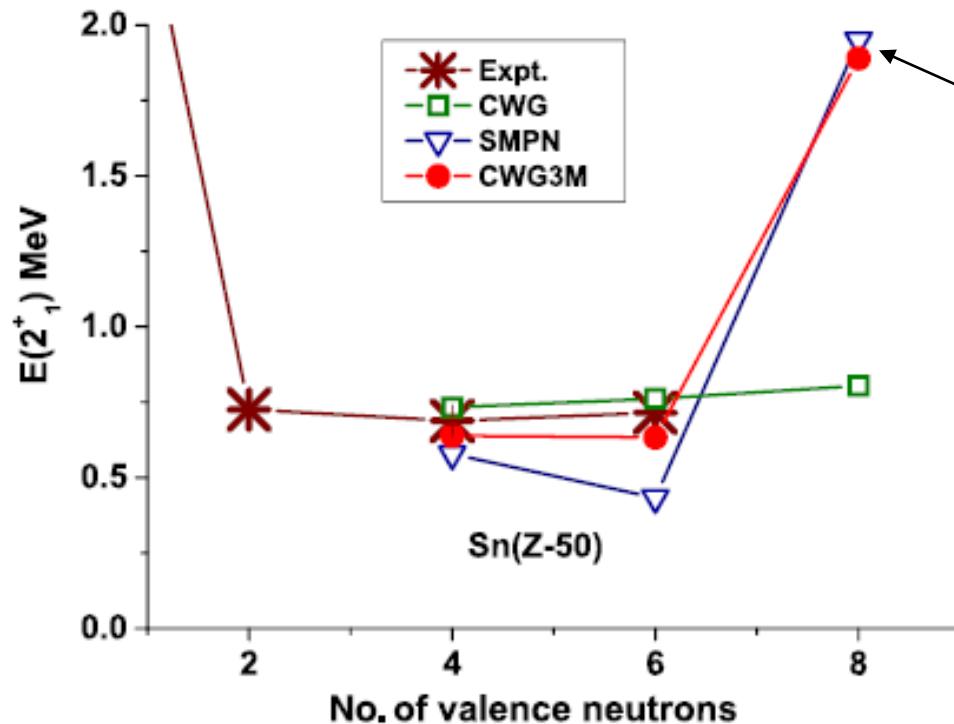
$[\pi g_{9/2}, \nu g_{7/2}] 2\text{QP } 1^+$ state

Comparison of the solar system r -process abundances in the $A \sim 130$ peak region with model predictions

$^{129-132}\text{Cd}$, ^{128}Pd , ^{122}Zr masses as well as the position and $\log(ft)$ values for 1^+ GT states in daughter nuclei are needed.

$T_{1/2}$ for waiting point ^{128}Pd — 3 1/s at IRINA

IRINA: Reducing pairing after N=82?



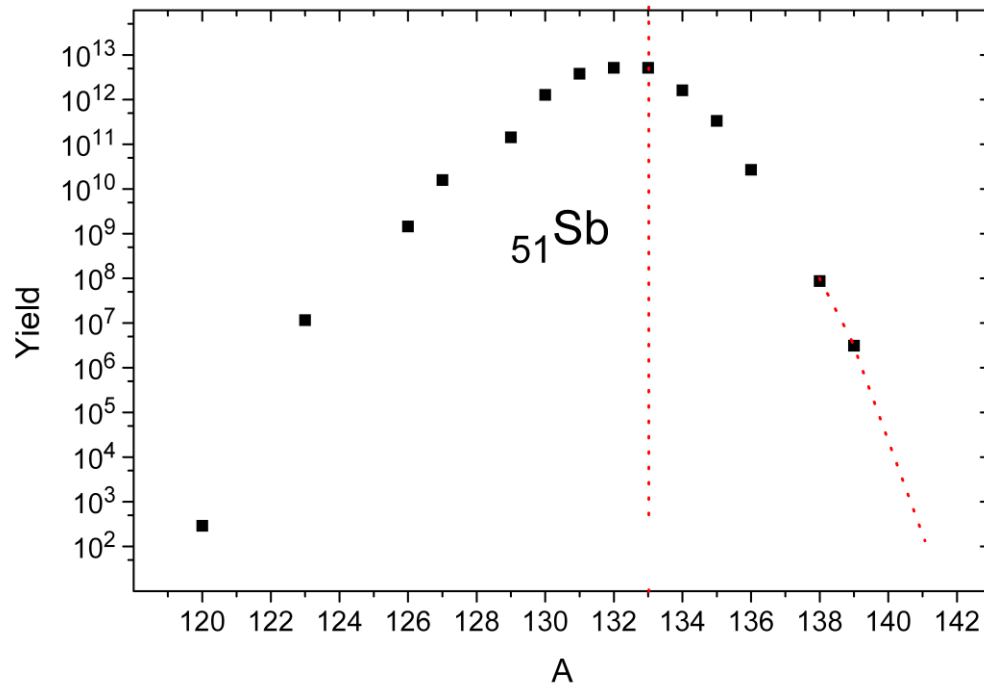
New magic number N=90?
Calculations with 3N forces

$^{136}\text{Te}^{84}$ puzzle: decrease of $E(2^+)$ without increase of $B(E2)$ — is described by decrease of pairing after N=82 caused by 3N forces

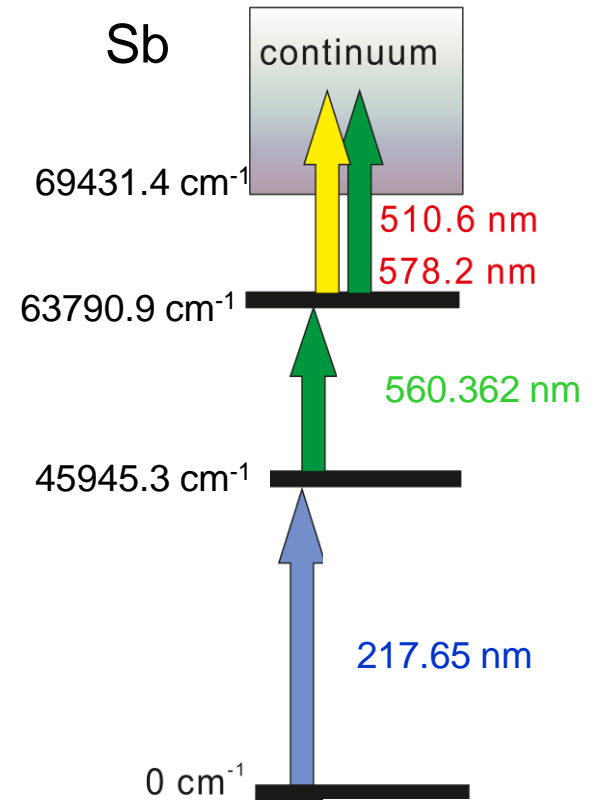
Description of $E(2^+)$ and $B(E2; 6^+ \rightarrow 4^+)$ for $^{136,138}\text{Sn}$ is better with 3N forces. Crucial will be the measurement of $B(E2; 2^+ \rightarrow 0^+)$ for ^{136}Sn . Predictions: 184 fm⁴ without 3N forces, 73 fm⁴ with 3N forces

^{136}Sn at IRINA: 10⁶ 1/s — RIB is necessary (for $B(E2)$)!

IRINA: Sb isotopic chain



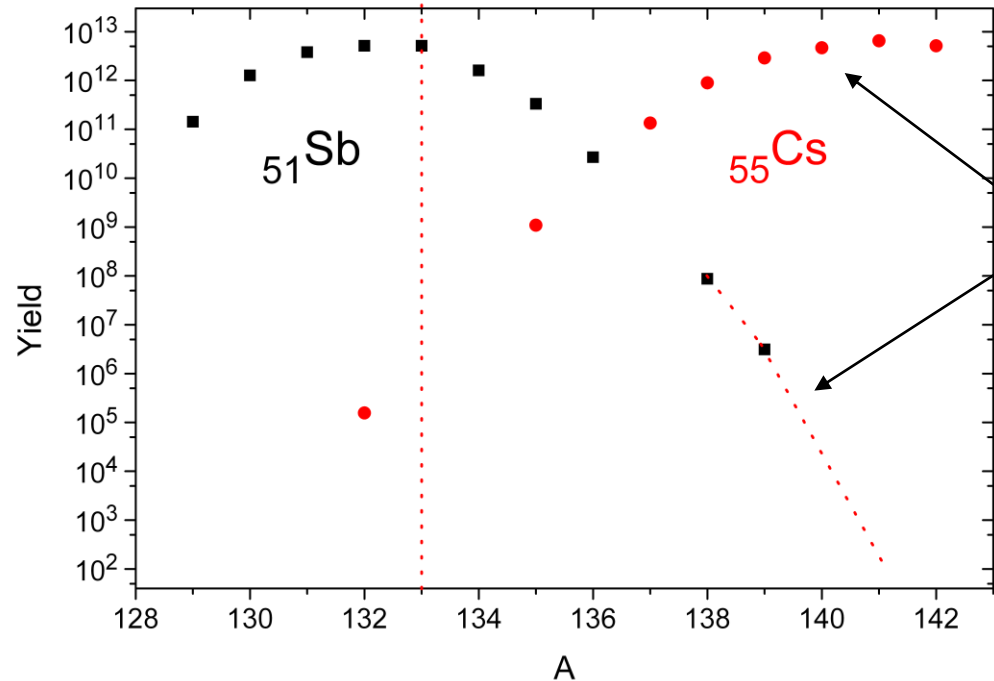
Single particle states near N=82, new N=90 magic number (?), shell effect at N=82...



At IRIS with 1-GeV protons ¹¹¹⁻¹³⁵Sb can be measured.

At IRINA this chain can be continued up to A=141.

IRINA: Sb isotopic chain

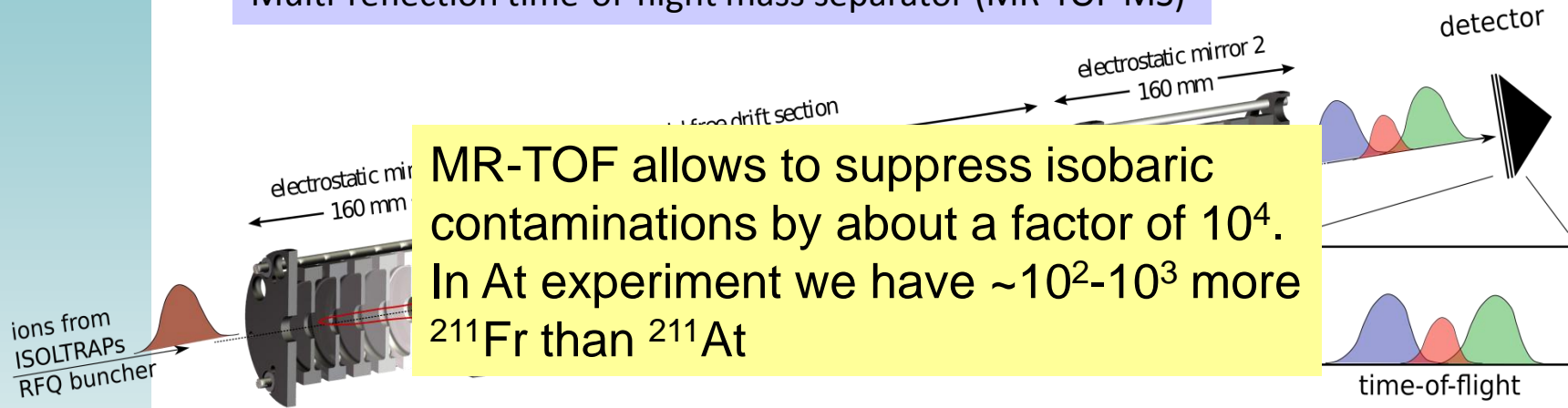


Cs background is 6 orders of magnitude greater than Sb yield!

At $A > 136$ neutrons from βn (? in ^{137}Sb $\beta n=49\%$) should be used for photo-ion current monitoring or/and background suppression

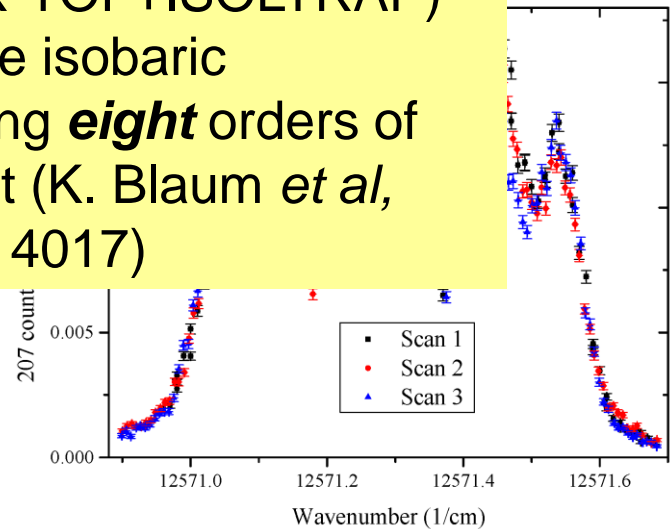
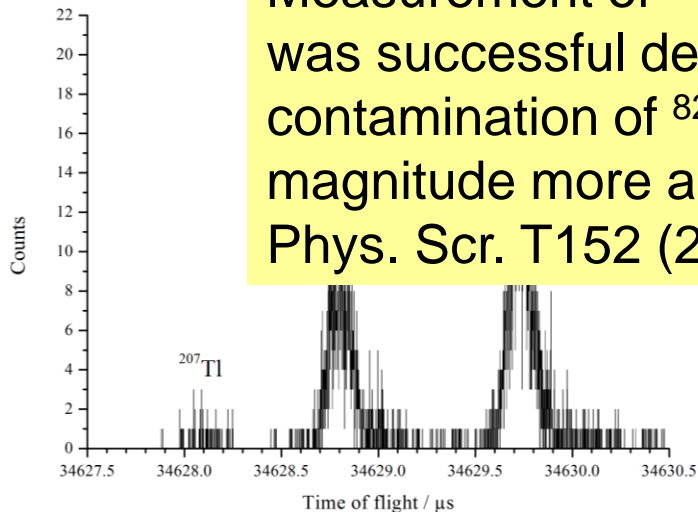
MR-TOF at ISOLDE

Multi-reflection time-of-flight mass separator (MR-TOF MS)

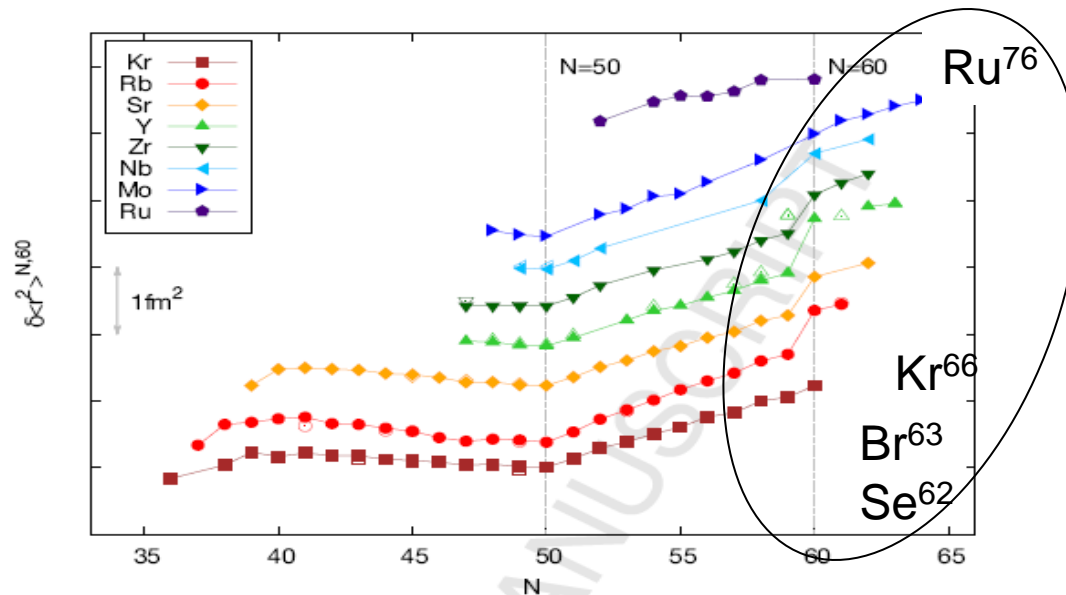


MR-TOF allows to suppress isobaric contaminations by about a factor of 10^4 . In At experiment we have $\sim 10^2$ - 10^3 more ^{211}Fr than ^{211}At

Measurement of ^{82}Zn (MR-TOF+ISOLTRAP) was successful despite the isobaric contamination of ^{82}Rb being **eight** orders of magnitude more abundant (K. Blaum *et al*, Phys. Scr. T152 (2013) 014017)



1. Onset of deformation near N=60



2. Octupole deformation at A~150 (Ba, Cs...)

3. Indium: high-spin isomers (21/2⁻, 29/2⁺), anomalous behaviour of μ for 1/2⁻ isomer, shell-effect at N=82

Previously measured Achievable at IRINA

104-127In⁵⁵⁻⁷⁸ \longrightarrow up to N=87

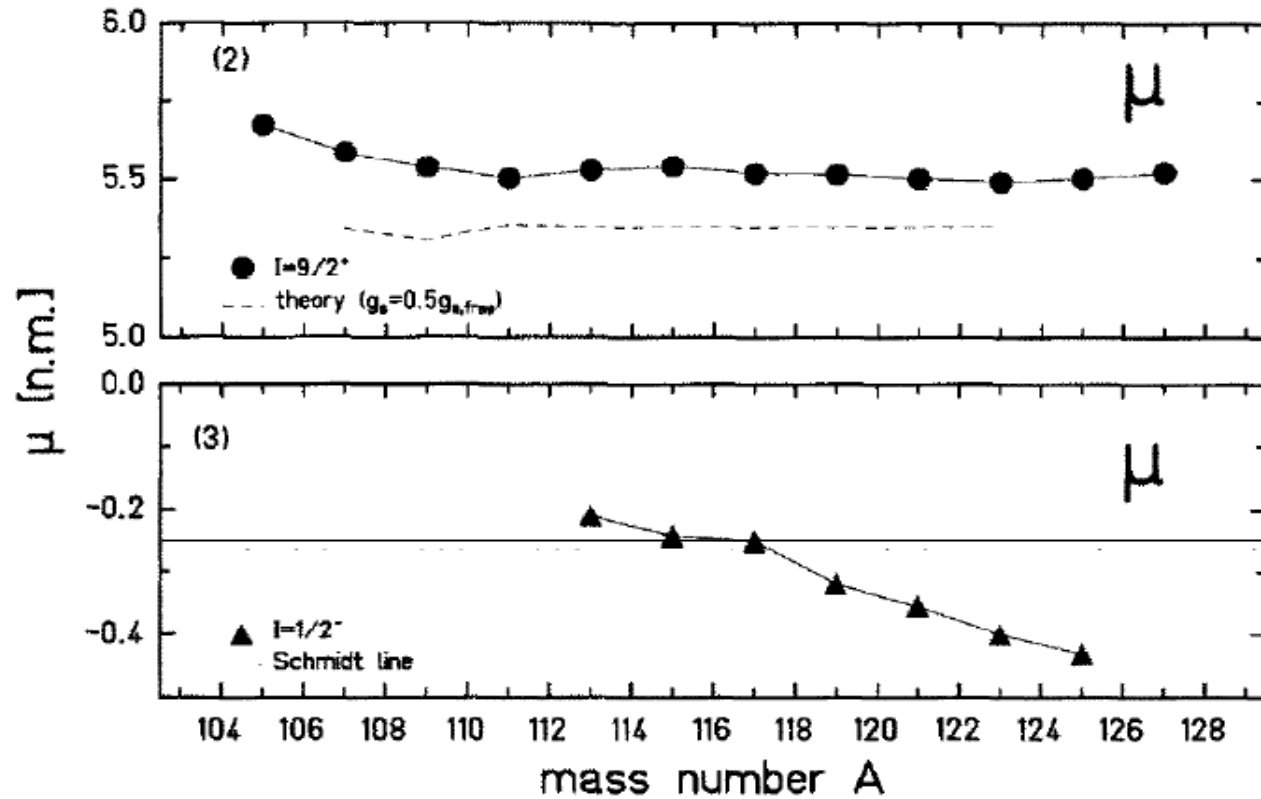
4.

IRINA: conclusions and outlook

Рекордные выходы n-избыточных ядер в диапазоне от ${}_{25}\text{Mn}$ до ${}_{68}\text{Er}$

1. Новая информация о $T_{1/2}$ и βn для моделирования r-процесса
2. Существование форм в области $28 < N < 40$, исчезновение подоболочки $N=40$
3. Уменьшение спаривания при $N < 82$, сжатие оболочечной щели при $N=82$ и $Z=28$ (?), влияние $3N$ сил (?)
4. Исчезновение оболочечного эффекта в зарядовых радиусах при $N=50$ (Ni) и $N=82$ (Sn): насколько правильно описываются спин-орбитальные силы в RMF? Влияние перераспределения одночастичных состояний?
5. Одночастичные состояния вблизи $N=50$, $Z=28$: влияние тензорных сил (?)
6. Одночастичные состояния вблизи $N=82$, $Z=50$: влияние тензорных сил (?)
7. Новое магическое число $N=90$ (?)
8. Использование MR-TOF и ПИТРАП для уменьшения фона
9. Квадрупольная деформация при $N > 60$, октупольная деформация вблизи $A=150$; классическая область деформации вблизи середины нейтронной оболочки ($N=104$); высокоспиновые изомеры в In

IRINA: In isotopes



No μ for high-spin isomers ($21/2^-$, $29/2^+$)